AIP Journal of Applied Physics

Structural evolution and optical properties of TiO 2 thin films prepared by thermal oxidation of sputtered Ti films

Chu-Chi Ting, San-Yuan Chen, and Dean-Mo Liu

Citation: Journal of Applied Physics **88**, 4628 (2000); doi: 10.1063/1.1309039
View online: http://dx.doi.org/10.1063/1.1309039
View Table of Contents: http://scitation.aip.org/content/aip/journal/jap/88/8?ver=pdfcov
Published by the AIP Publishing

Articles you may be interested in
Electrical and optical properties of Nb-doped TiO 2 films deposited by dc magnetron sputtering using slightly reduced Nb-doped TiO 2 x ceramic targets
J. Vac. Sci. Technol. A **28**, 851 (2010); 10.1116/1.3358153

Structural, electrical, optical, and photoelectrochemical properties of thin titanium oxinitride films (Ti O 2 2 x N x with 0 x 1)
J. Vac. Sci. Technol. A **24**, 2199 (2006); 10.1116/1.2362740

Optical properties of TiO 2 thin films estimated by photothermal deflection spectroscopy
Rev. Sci. Instrum. **74**, 863 (2003); 10.1063/1.1517149

Nonlinear optical absorption in undoped and cerium-doped BaTiO 3 thin films using Z -scan technique
Appl. Phys. Lett. **76**, 1003 (2000); 10.1063/1.125920

TiO 2 electrochromic thin films by reactive direct current magnetron sputtering
J. Vac. Sci. Technol. A **15**, 2673 (1997); 10.1116/1.580941

Re-register for Table of Content Alerts

Create a profile.
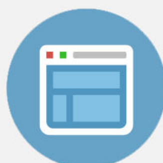
Sign up today!

[This article is copyrighted as indicated in the article. Reuse of AIP content is subject to the terms at: http://scitation.aip.org/termsconditions. Downloaded to] IP: 140.113.38.11 On: Thu, 01 May 2014 07:41:17

JOURNAL OF APPLIED PHYSICS VOLUME 88, NUMBER 8 15 OCTOBER 2000

Structural evolution and optical properties of TiO_2 thin films prepared by thermal oxidation of sputtered Ti films

Chu-Chi Ting and San-Yuan Chen
Department of Materials Science and Engineering, National Chiao-Tung University, Hsinchu, Taiwan 300, Republic of China

Dean-Mo Liu
Department of Metals and Materials Engineering, The University of British Columbia, #309-6350 Stores Road, Vancouver, British Columbia V6T 1Z4, Canada

(Received 8 July 1999; accepted for publication 13 July 2000)

A dense rutile TiO_2 thin film was synthesized by the thermal oxidation of a sputtered titanium metal film in ambient air. The effects on optical properties of TiO_2 films of the crystal structure and microstructural evolution at various oxidation temperatures were investigated. The Ti films transformed into single-phase rutile TiO_2 at temperatures $\geqslant 550\,°C$ without going through an anatase-to-rutile transformation. Instead, an additional crystalline Ti_2O phase was detected at 550 °C only. An increase in the oxidation temperatures ranging between 700 and 900 °C led to an increase in both the refractive index and absorption coefficient, but a decrease in the band gap energy (E_g). According to the coherent potential approximation model, the band gap evolution of the oxidized films was primarily attributed to the electronic disorder due to oxygen deficiency at a higher oxidation temperature rather than the presence of an amorphous component in the prepared films. © *2000 American Institute of Physics.* [S0021-8979(00)07920-2]

I. INTRODUCTION

Titanium dioxide has been extensively studied in recent decades.[1–3] Its remarkable optical and electronic properties have received considerable attention for optoelectronic applications. Several techniques including chemical vapor deposition, spray pyrolysis, sol–gel coating, and rf magnetron sputtering have been developed for TiO_2 thin films fabrications. The TiO_2 films prepared from these techniques exhibit a wide variety of structures and optical properties.[4–8]

Three crystallographic modifications occur in TiO_2: brookite, anatase, and rutile. The former two modifications are thermodynamically unstable, while the latter is stable. The rutile phase has a greater density ($\rho = 4.25\,g/cm^3$) and refractive index ($n = 2.75$ at $\lambda = 550\,nm$) than the anatase phase ($\rho = 3.89\,g/cm^3$ and $n = 2.54$ at $\lambda = 550\,nm$). Generally, TiO_2 films were deposited by a reactive rf magnetron sputtering with controlled partial pressures of Ar and O_2. Prior to a postdeposition annealing, the as-deposited TiO_2 film exhibits an amorphous structure. However, it transforms into a mixture of anatase and rutile phases at 700–900 °C annealing, a temperature regime essential for the anatase–rutile transformation to occur.[9] A higher annealing temperature is normally required to achieve single-phase rutile.[10–12]

The optical properties of TiO_2 thin films have been extensively investigated.[13–16] A postdeposition annealing of TiO_2 films leads to densification of the deposited layers, accompanied by a microstructural coarsening (i.e., grain growth and phase transformation). Therefore, a decrease in optical transmittance and an increase in refractive index of the TiO_2 thin films are frequently observed as annealed at higher temperatures.[13,16] In addition to the optical properties, several attempts (e.g., by doping) have been employed to reduce the band energy of TiO_2 to a level allowing a better quantum yield upon photon–electron conversions.[17,18]

A very simple method has been employed by means of a direct exposure of Ti metal film to thermal oxidation for the fabrication of TiO_2 film in this study. The sputtered Ti film was easily transformed to single rutile phase at temperatures as low as 550 °C in air, without going through an anatase-to-rutile phase transformation. Therefore, optical properties such as transmittance ($T\%$), refractive index (n), absorption coefficient (α), and optical band gap (E_g) of the resulting TiO_2 films were systematically examined in terms of the structural evolution of the sputtered Ti films after high-temperature oxidation at various temperatures.

II. EXPERIMENTAL PROCEDURE

Titanium films were prepared using a dc magnetron sputtering system having a 30 dm^3 cylindrical stainless-steel chamber. The target was a titanium disk (purity 99.6%). The titanium was deposited at a constant dc power of 50 W onto a quartz substrate under a background pressure of 5×10^{-6} Torr. A target–substrate distance was kept at a constant of 70 mm. During this operation, an ultrahigh purity (99.999%) Ar gas was used. Under a sputtering pressure of 8 mTorr, the sputtering time was 15 min and the substrate was maintained at room temperature. Prior to each experiment, the target was presputtered in an argon atmosphere (99.999% purity) for 8 min to remove surface oxides on the target. The as-deposited Ti films (a thickness of ~170 nm) were subjected to postdeposition annealing at temperatures ranging between 400 and 1000 °C for 1 h in air.

An UV–visible spectrophotometer (Hitachi, UV-3410) was used to characterize the optical properties of the result-

 © 2000 American Institute of Physics

[This article is copyrighted as indicated in the article. Reuse of AIP content is subject to the terms at: http://scitation.aip.org/termsconditions. Downloaded to] IP: 140.113.38.11 On: Thu, 01 May 2014 07:41:17

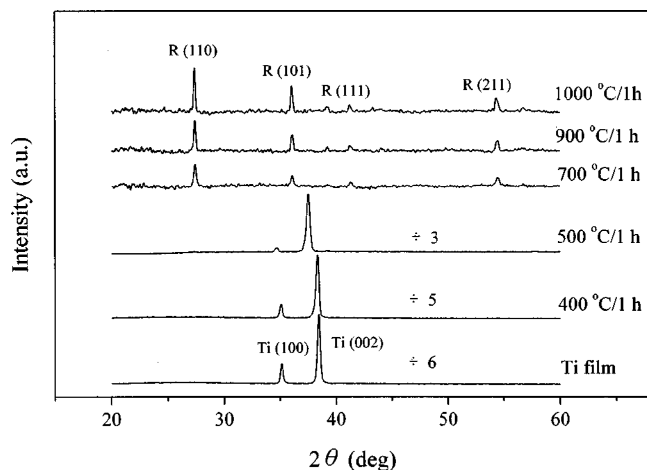

FIG. 1. X-ray diffraction patterns of Ti film and Ti films oxidized in air at different temperatures.

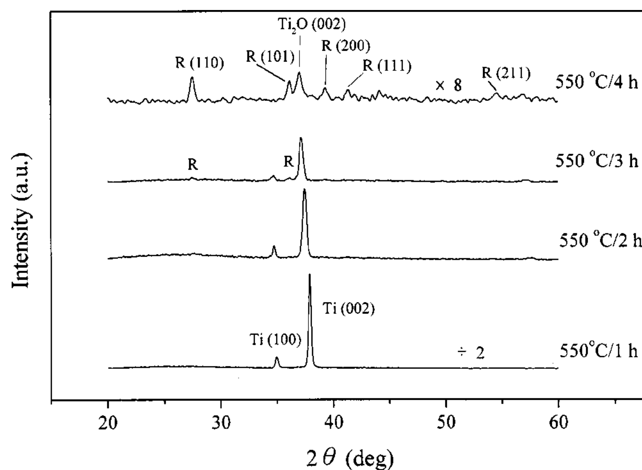

FIG. 2. X-ray diffraction patterns for Ti films following oxidation at 550 °C for various time periods.

ing TiO_2 thin films. the crystal structure was determined by x-ray diffraction (XRD) (MAC Science, M18X). Scanning electron microscopy (Hitachi, S4000) was used for microstructural examination. The thickness of Ti film and the resulting TiO_2 films was measured by a surface profiler (Sloan, Dektak^{3}ST). Following annealing, the stoichiometry of the films was performed by a Rutherford backscattering spectroscopy (RBS). The resistivity of the TiO_2 films was obtained from the current–voltage measurements of the Pt–TiO_2–Pt structures with a HP4156B semiconductor parameter analyzer.

The volume fraction of amorphous (f_A) and rutile (f_R) phases in the TiO_2 films was determined according to the method described by DeLoach *et al.*[19] Briefly, the volume fraction of one component, rutile, in an uniform mixture is related to the integrated intensity of a specific reflection, $I_{(110)}$. The selection of a ''standard'' pure rutile film has to be strictly limited to the one with an identical preferred orientation as the film state to be analyzed. In this case, the films annealed at 1000 °C were found to be entirely of the rutile phase, which was used as the standard rutile film for further determination of the rutile volume fraction of TiO_2 films under different oxidation conditions. The f_R was defined as $[I_{(110)}/I_{S(110)}]$ for other film states, where $I_{S(110)}$ is the integrated intensity of the standard rutile film. Once the f_R was determined, the volume fraction for the amorphous phase (f_A) equaled $1-f_R$.

III. RESULTS AND DISCUSSION

A. Crystal structure

Figure 1 shows the XRD patterns of the Ti films oxidized in air for 1 h at various temperatures. When the temperature was increased from 400 to 500 °C, a shift to the low angle of the Ti (002) peak was clearly observed. This progressively low-angle shift indicated an enlargement of the lattice volume via the incorporation of oxygen atoms from ambient air. Until annealed at 700 °C, a single rutile phase appeared. The XRD patterns reveal two interesting features. The formation of a single rutile phase TiO_2 at 700 °C, which is several hundred degrees lower (generally near or greater than 900 °C) than formations synthesized from other methods.[10,11,16] The other feature is the appearance of an amorphous phase. As evidenced from XRD patterns, all peaks presented lower intensities at 700 °C, implying the coexistence of amorphous titanium oxide with crystalline rutile. A further increase to 1000 °C resulted in an increase in diffraction intensity with an associated decrease in the amorphous background of the XRD patterns, indicating an improved crystallinity of the films.

Notably, anatase TiO_2 was never detected in this investigation, especially when subjected to the temperature range, 700–1000 °C, (where the anatase-to-rutile phase transformation would occur).[10,11,13] A possible explanation is the formation of significant quantity of oxygen vacancies in the oxidized film, known as the Mageli phase, which is known to markedly accelerate the anatase-to-rutile transformation.[20] However, this explanation appears unconvincing, simply because traces of anatase TiO_2 are undetectable. To further elucidate the phase evolution, the Ti film was annealed at 550 °C for various time periods. Figure 2 indicates that, again, traces of anatase TiO_2 were undetected. Instead, the XRD pattern displays a mixture of rutile TiO_2 and Ti_2O phases at 4 h annealing. Following further annealing, the Ti_2O phase is thermodynamically unstable and transformed to rutile structure. According to a study by Padma *et al.*[21] layered structures of several Ti–O intermediate oxides are generated from the surface to the interior of the film. However, other oxides[22] such as Ti_3O_5, Ti_2O_3, and TiO were undetected. In Fig. 2, an appreciable quantity of the amorphous phase was observed in the XRD patterns when annealed at 550 °C for 4 h. This amorphous phase was also observed at higher temperatures (Fig. 1). Suhail *et al.*[13] reported a similar phenomenon in TiO_2 films prepared via dc reactive magnetron sputtering.

The RBS analysis of the stoichiometry of the films, annealed at 700–900 °C, revealed an O/Ti atomic ratio of 2. It was strongly believed that oxygen vacancies may also develop, but such a relatively small concentration was probably beyond the resolution, approximately 0.5%, of RBS analysis.

[This article is copyrighted as indicated in the article. Reuse of AIP content is subject to the terms at: http://scitation.aip.org/termsconditions. Downloaded to] IP: 140.113.38.11 On: Thu, 01 May 2014 07:41:17

TABLE I. Evolution of phase composition (f_R and f_A) and FWHM at (110) peak of the TiO_2 films prepared at different oxidation temperatures for 1 h.

Temperature (°C)	f_R	f_A	Diffraction angle (2θ) at rutile (110) peak	FWHM (deg.) of rutile (110) peak
700	86.6	13.4	27.453	0.2358
800	89.5	10.5	27.451	0.1906
900	90.5	9.5	27.447	0.1856
1000[a]	100	0	27.421	0.1716

[a]The film oxidized at 1000 °C under ambient air presented an entire or predominant rutile phase and was applied as a standard film for the determination of phase composition in other oxidized films.

TABLE II. Lattice parameters (a and c) of the rutile TiO_2 films oxidized at different temperatures, with the parameters of bulk single-crystal rutile TiO_2.

Temperature (°C)	a(Å)	c(Å)
700	4.5863	2.9560
900	4.5892	2.9561
1000[a]	4.5925	2.9586
Single crystal	4.5933	2.9592

[a]At 1000 °C, the optical transmittance of the film is too weak and a further analysis of optical properties cannot be accurately determined by Swanepoel's method.

This implies that the amorphous phase may have an O/Ti ratio relatively close to the crystalline (rutile TiO_2) phase. This finding seems unexplainable as, in the presence of an appreciable amount of suboxide layers, an overall O/Ti ratio must be substantially smaller than 2. Therefore, one possibility is a significant shortening of the oxidation time to reach a near-stiochoimetric ratio under the experimental control.

A study by Rogers *et al.*[23] verified that the TiO_2 phase growth rate heavily depends on temperature. According to this four-layer model, it is possible to estimate the thickness of the TiO_2 layer (the first layer adjacent to the oxygen atmosphere) upon thermal oxidation in our films. Based on oxygen mass balance and Fick's diffusion law, the change in the layer thickness (h) of TiO_2 on oxidation, at time t, can be formulated as

$$\frac{dh}{dt}=\frac{AD^{1/2}}{(t^{1/2})2(1-W)}, \tag{1}$$

where D is the effective oxygen diffusion coefficient, W is the mass fraction of oxygen, and A is the surface area exposed to oxygen.

Following rearrangement and integration, the thickness (h) can be estimated by

$$h=\frac{A(Dt)^{1/2}}{2(1-W)}. \tag{2}$$

Equation (2) is a parabolic expression representing the growth of the TiO_2 layer upon oxidation, and it is assumed this relationship is valid for the current system where the oxygen partial pressure is 0.2 atm. Following a substituting of the appropriate values ($A=1\ \mathrm{cm}^2$, $W=0.36$, D which is estimated to be the order of $10^{-12}\ \mathrm{cm}^2/\mathrm{s}$ at 700 °C, and $t=3600\ \mathrm{s}$) into Eq. (2), the calculated h is 468 nm, (which is considerably thicker than the sputtered Ti film). In fact, Rogers *et al.*[23] suggested that the diffusion coefficient D should be greater than the estimated value, ($10^{-12}\ \mathrm{cm}^2/\mathrm{s}$), at 700 °C. This finding implies that a thickness greater than 468 nm is expected. Furthermore, a preferential path for the oxygen diffusion along the grain boundary (or through defect structures in the amorphous phase) of the polycrystalline TiO_2 film should also increase the oxidation rate. Therefore, we can infer that the Ti film was completely converted to a near-stoichiometric TiO_2 film at 700 °C (and above) within 1 h under ambient oxygen partial pressure. This may be the major reason for the absence of other oxides. The films oxidized at 550 °C were essentially oxygen nonstoichiometric and associated with the formation of a sufficient quantity of oxygen vacancies.

For a low-temperature oxidation, a longer period is required for the transformation of Ti to TiO_2 as a result of slower oxygen diffusion kinetics,[23] as evidenced by the presence of a crystalline Ti_2O in Fig. 2. Further oxidation at higher temperatures promotes crystallization of the amorphous phase, resulting in an increase in both the quantity (f_R) and crystallinity (represented by a decreased full width at half maximum, FWHM) of the rutile phase (Table I).

Table II lists the lattice parameters of the oxidized films calculated for different temperatures. The lattice parameters of single-crystal rutile TiO_2 are also tabulated. Obviously, the lattice constants of the rutile TiO_2 films increased with temperature and tended towards the single-crystal values, which corresponds to the findings in Table I. This seems consistent with previous XRD analysis (Fig. 1). The crystal structure of the oxidized films tends towards that of single-crystal rutile with increasing temperature, which further suggests a better arrangement of O and Ti atoms in the rutile crystals.

B. Film morphology

Figure 3 illustrates the microstructural evolution of the films oxidized at different temperatures. The average grain size of the Ti film presented in Fig. 3(a) is approximately 60 nm prior to oxidation. As the temperature was raised to 700 °C, the TiO_2 film did not significantly alter the grain size, which has an average size of approximately 58 nm [Fig. 3(b)]. However, the grain size rapidly increases to ~100 nm at 800 °C and to ~155 nm at 900 °C [Figs. 3(c) and 3(d)]. The microstructure of the films oxidized at 700 °C is relatively homogeneous in comparison to films oxidized at 800 and 900 °C (where some larger grains can be seen). This finding suggests that these films are essentially inhomogeneous and, therefore, a higher surface roughness can be expected. With increasing temperature, some small voids are present and enlarge. The presence of these small voids within the film structure provides alternative but direct conduits for the access of oxygen molecules flowing inward from the ambient environment, supporting the hypothesis of an increasing oxidation rate as discussed in the previous section.

[This article is copyrighted as indicated in the article. Reuse of AIP content is subject to the terms at: http://scitation.aip.org/termsconditions. Downloaded to] IP: 140.113.38.11 On: Thu, 01 May 2014 07:41:17

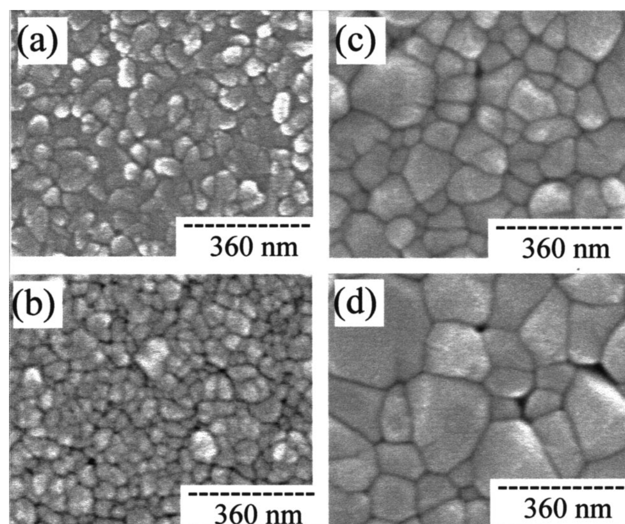

FIG. 3. Microstructural evolution of (a) as-deposited Ti film, and following oxidation at (b) 700 °C, (c) 800 °C, and (d) 900 °C.

C. Optical properties

Figure 4 shows the spectra of optical transmittance of the TiO_2 films annealed at different temperatures. The poorest transmittance, especially in the visible region, occurs at 550 °C/4 h, suggesting the presence of a sufficient amount of oxygen vacancies that have significantly absorbed the incident light.[24,25] This finding seems consistent with the XRD patterns illustrated in Fig. 2, indicating that the film following a 550 °C/4 h oxidation is oxygen deficient. The optical transmittance can be significantly improved while increasing the oxidation temperature to 700 °C. However, it decreases at 800 and 900 °C. In this case, the optical transmittance is also accompanied by an appreciable blueshift of the spectrum in the lower wavelength region. Suhail *et al.*[13] and other related reports attributed (albeit not unambiguously) these results to several possibilities, primarily anatase–rutile transformation, films densification, and the partial reduction of TiO_2 films at high temperatures. However, since such a phase transformation was undetected between 700 and 900 °C, an enhanced crystallinity (amorphous→crystalline) of the rutile phase with increasing temperature may be one of the major causes under current investigation.

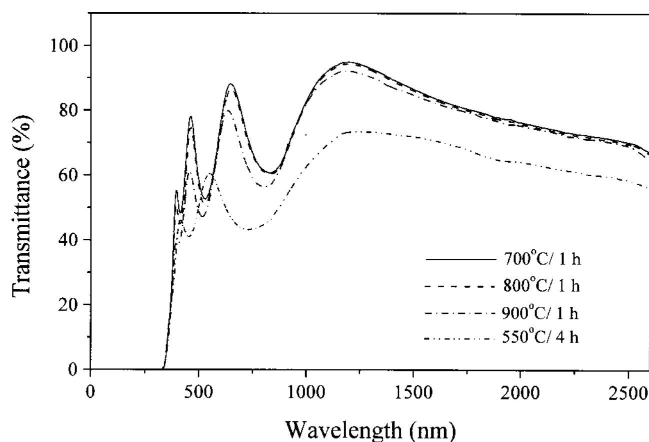

FIG. 4. Optical transmittance ($T\%$) of the TiO_2 films, prepared by oxidizing at different temperatures, as a function of wavelength.

Additionally, since the enthalpy (ΔH_s) of oxygen vacancy formation (n_s) in TiO_2 is endothermic,[26]

$$TiO_2 + \Delta H_s \rightarrow TiO_{2-x} \quad (3)$$

the population of the vacancy can be enhanced with increasing temperature as

$$n_s = N_s \exp(-\Delta H_s/2kT), \quad (4)$$

where N_s is the maximum number of sites per m^3 to form Schottky defects, k the Boltzmann constant (1.38×10^{-23} J/K), and T the absolute temperature. By substituting $\Delta H_s = 5 \times 10^{-19}$ J, we obtain $n_s/N_s = 4.6 \times 10^{-8}$ at 700 °C and 6.6×10^{-7} at 900 °C, over an order of magnitude greater in concentration than that at 700 °C. The actual population of the oxygen vacancies can be higher than the calculated values due to the incorporation of impurities originated from both target materials and environment; however, it is difficult to quantify precisely. An earlier study by Blumenthal *et al.*[27] revealed that an oxygen deficiency can be extended to TiO_{2-x} with $x = 0.01$ (a value relatively close to the limit of maximum resolution of the RBS analysis) via annealing TiO_2 between 900 and 1000 °C. When this is applied to our films, the concentration of oxygen defect will be 3.19×10^{14} per m^3, much greater than the above calculation. Therefore, we believe that the oxygen vacancy should play a role in the observed spectra. The influence of microstructural coarsening on light scattering can be ignored as the transmittance displayed a similar trend in the longer wavelength region as observed in the short wavelength region. Obviously, an appreciable blueshift and the decrease of the transmittance maximum in the low wavelength region at 900 °C suggest the presence of an appreciable quantity of oxygen defects,[24,25] which is qualitatively consistent with that described in Eq. (4). In addition, the resistivity of the TiO_2 films postannealed at 900 °C for 1 h increased from 2×10^9 to $1 \times 10^{10}\ \Omega$ cm under 0.2 atm oxygen (air) ambient and 1 atm oxygen ambient, respectively. These values are much lower than the resistivity of single-crystal rutile (having a value of $\sim 10^{20}\ \Omega$ cm at room temperature[28]), suggesting that the increased electrical conductivity of the prepared TiO_2 films is due to electronic disorder caused by the oxygen nonstoichiometry.[29–32] Since the oxygen vacancies can be compensated by postannealing in oxygen ambient,[33,34] the resistivity of the TiO_2 films can increase under a higher oxygen gas pressure. Therefore, it is strongly believed that there really exists an appreciable quantity of oxygen vacancies in the TiO_2 film annealed at 900 °C/1 h in air.

Figures 5(a) and 5(b) illustrate the refractive index (n) and absorption coefficient (α) (as a function of wavelength) of the films oxidized at different temperatures, which were derived from the transmittance spectra using Swanepoel's method.[35] The increase in both n and α of the films with raising annealing temperature (which is consistent with previous investigations[11,13,16]) was considered as a result of the increases in compactness, crystallinity and oxygen defects of the rutile TiO_2 films.

[This article is copyrighted as indicated in the article. Reuse of AIP content is subject to the terms at: http://scitation.aip.org/termsconditions. Downloaded to] IP: 140.113.38.11 On: Thu, 01 May 2014 07:41:17

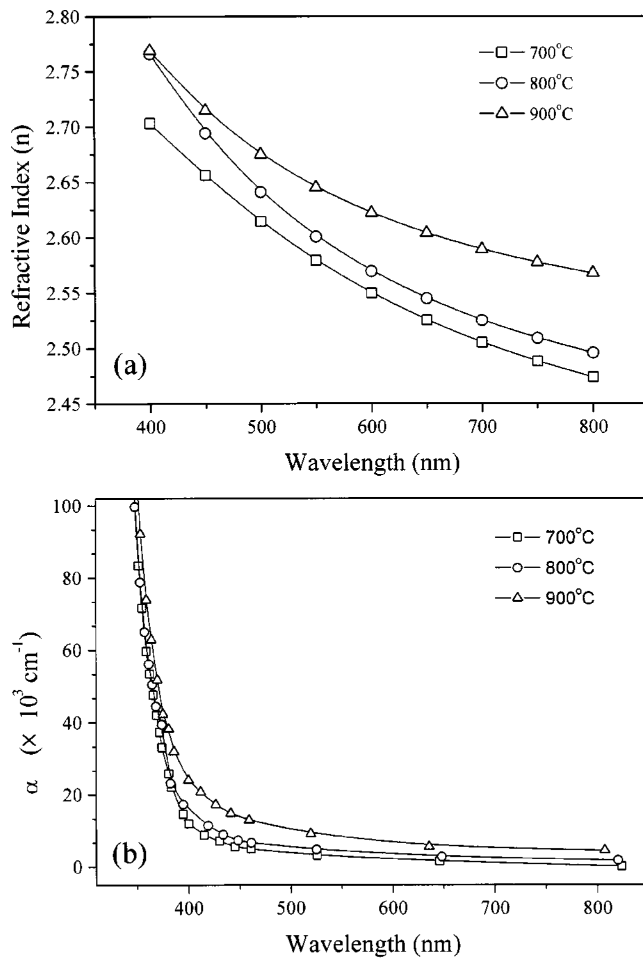

FIG. 5. Effect of oxidation temperature on (a) refractive index and (b) absorption coefficient of the TiO_2 films, in terms of wavelength.

The optical band gap (E_g) of the TiO_2 films can be related to absorption coefficient (α) by

$$\alpha h\nu = \mathrm{const}(h\nu - E_g)^2. \tag{5}$$

Figure 6 plots the relationship of $(\alpha h\nu)^{1/2}$ versus photon energy (E) of the rutile TiO_2 films and the extrapolated optical band gaps of the films were determined. When the temperature is increased from 700 to 900 °C, the value of E_g decreased from 3.20 to 3.12 eV.

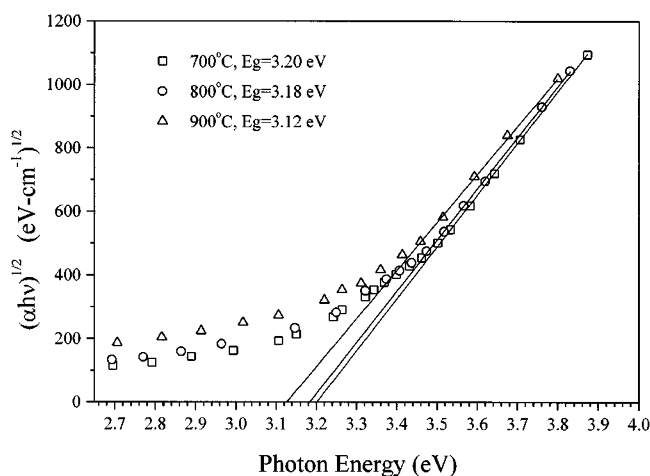

FIG. 6. $(\alpha h\nu)^{1/2}$ as a function of photon energy for the TiO_2 films prepared by oxidation at different temperatures.

Similar band energy evolution has also been noticed in several thin films including TiO_2[12,13,16] and perovskite materials such as $BaTiO_3$.[36] Martin *et al.*[16] assumed that such an evolution in TiO_2 films might be a result of the variation of density and structural modifications. They also ascribed this evolution to the electronic disorder induced by oxygen nonstoichiometry in sputtered films. Vasantkumar *et al.*[37] inferred the decrease in the band gap energy with increasing temperature to be due to the lowering of interatomic spacing (amorphous→crystalline). This was later confirmed experimentally by Lu *et al.*[36] in their study of $BaTiO_3$ applying the band gap model proposed by Harrison.[38] However, in our films the interatomic spacing increases (Table II) (rather than decreased as appeared in perovskite materials), with an increasing temperature. The band gap energy of our films cannot be accounted for in relation to Harrison's model,[38] which obviously contradicts current observations. Instead, following the model proposed by DeLoach *et al.*[19] [based on the framework of coherent potential approximation (CPA) model], the optical band gap of a rutile polycrystalline film is directly related to the structural and electronic disorders. However, their study demonstrated only structural disorder due to the presence of a substantial quantity (30 vol %) of an amorphous component. The band energy for those disordered crystal films (i.e., virtual rutile crystal) can be modeled by a generalized equation

$$E_g(W,T) = 3.22\ \mathrm{eV} - 3.14\ E_0(W,T), \tag{6}$$

where E_g is the optical band gap of the disordered crystal and E_0 the reverse slope of the exponential region (i.e., electronic disorder), which is proportional to W^2/B (where W is an energy term, increasing with structural and compositional disorder, and B is the sum of the valence and conduction band half widths). The value 3.22 eV is the band energy for a virtual rutile phase. According to Eq. (6), a structural disorder introduced by an amorphous component would increase the value of E_0 and causes a decrease in E_g. However, their model cannot account for the variation of E_g in this study if based solely on structural disorder, as the values of E_g (designated in Fig. 6) decreased with decreasing f_A, [i.e., increasing structural disorder (Table I)]. Therefore, based on the framework of Eq. (6), the primary plausible reason for this discrepancy results from electronic disorder, that is, oxygen nonstoichiometry. Namely, the electronic disorder resulting from oxygen deficiency dominates the band gap evolution rather than that induced solely by structural disorder for the films prepared in this study. The E_0 calculated values based on Eq. (6) together with the band energy values (in Fig. 6) demonstrate $E_0 = 6.37\times10^{-3}$ eV at 700 °C, $E_0 = 1.27\times10^{-2}$ eV at 800 °C, and $E_0 = 3.18\times10^{-2}$ eV at 900 °C, which indicates an increased electronic disorder with increasing temperature. This finding is not only qualitatively consistent with the CPA model described in Eq. (6) but also provides alternative support for the argument revealed by Martin *et al.*[16]

[This article is copyrighted as indicated in the article. Reuse of AIP content is subject to the terms at: http://scitation.aip.org/termsconditions. Downloaded to] IP: 140.113.38.11 On: Thu, 01 May 2014 07:41:17

IV. CONCLUSION

This study investigated the structural evolution and optical properties of TiO_2 thin film prepared by thermal oxidation of sputtered Ti film over temperatures ranging between 700 and 900 °C. A polycrystalline rutile TiO_2 phase, accompanied by an appreciable quantity of an amorphous phase, can be obtained at a temperature as low as 550 °C. High-temperature oxidation results in an increase in the crystallization, refractive index, and absorption coefficient, but a decreased band gap energy of rutile TiO_2 films. Although the RBS analysis cannot accurately estimate the stoichiometry of the oxidized films, the argument based on the coherent potential approximation implies that the electronic disorder due to the formation of oxygen defect in the oxidized films is principally responsible for the observed band gap evolution at temperatures ranging between 700 and 900 °C. Conversely, the influence of the amorphous component is less significant in these films.

ACKNOWLEDGMENTS

The authors would like to thank the National Science Council of the Republic of China for financially supporting this research under Contract No. NSC-87-2218-E-009-016. Dr. H. Y. Lee and Dr. H. S. Sheu from the Synchrotron Radiation Research Center are appreciated for their helpful discussions. Professor B. X. Qiu is also commended for assistance with the optical measurements.

[1] Y. Lida and S. Ozaki, J. Am. Ceram. Soc. **44**, 120 (1961).
[2] G. P. Burns, J. Appl. Phys. **65**, 2095 (1965).
[3] J. Yang and J. M. F. Ferreira, MRS Bull. **33**, 389 (1998).
[4] K. N. Rao, M. A. Murthy, and S. Mohan, Thin Solid Films **176**, 181 (1989).
[5] E. Ritter, J. Vac. Sci. Technol. **6**, 225 (1966).
[6] J. R. McNeil, G. A. Al-Jumaily, K. C. Jungling, and A. C. Barron, Appl. Opt. **24**, 486 (1985).
[7] S. Schiller, G. Beister, W. Sieber, S. Schirmer, and E. Hacker, Thin Solid Films **83**, 239 (1981).
[8] L. F. Donaghey and K. G. Geraghty, Thin Solid Films **38**, 271 (1976).
[9] G. J. Exarhos, J. Vac. Sci. Technol. A **4**, 2962 (1986).
[10] P. Löbl, M. Huppertz, and D. Mergel, Thin Solid Films **251**, 72 (1994).
[11] C. J. Ting, S. Y. Chen, and D. M. Liu, presented at the 101st Annual Meeting of the American Ceramic Society, Indianpolis, IN, 25–28 April, 1999.
[12] N. Martin, C. Rousselot, D. Rondot, F. Palmino, and R. Mercier, Thin Solid Films **300**, 113 (1997).
[13] M. H. Suhail, G. M. Rao, and S. Mohan, J. Appl. Phys. **71**, 1421 (1992).
[14] L. J. Meng and M. P. dos Santos, Thin Solid Films **226**, 22 (1993).
[15] W. G. Lee, S. I. Woo, J. C. Kim, S. H. Choi, and K. H. Oh, Thin Solid Films **237**, 105 (1994).
[16] N. Martin, C. Rousselot, C. Savall, and F. Palmino, Thin Solid Films **287**, 154 (1996).
[17] G. Blondeau, M. Froelicher, M. Froment, A. Hugot-Le Goff, and J. Zerbino, J. Electrochem. Soc. **126**, 1592 (1979).
[18] M. Guglielmi, P. Colombo, V. Rigato, R. Battaglin, A. Boscolo-Boscoletto, and A. DeBattisti, J. Electrochem. Soc. **139**, 1655 (1992).
[19] J. D. DeLoach, G. Scarel, and C. R. Aita, J. Appl. Phys. **85**, 2377 (1999).
[20] R. D. Shannon and J. A. Pask, J. Am. Ceram. Soc. **48**, 391 (1965).
[21] R. Padma, K. Ramkumar, and M. Satyam, J. Mater. Sci. **23**, 1591 (1988).
[22] *Phase Diagrams for Ceramists*, edited by E. M. Levin, C. R. Robbins, H. F. McMurdie, and M. K. Reser (American Ceramic Society, Columbus, OH, 1964), p. 41.
[23] J. W. Rogers, Jr., K. L. Erickson, D. N. Belton, R. W. Springer, T. N. Taylor, and J. G. Beery, Appl. Surf. Sci. **35**, 137 (1989).
[24] F. Zhang, Z. Zheng, X. Ding, Y. Mao, Y. Chen, Z. Zhou, S. Yang, and X. Liu, J. Vac. Sci. Technol. A **15**, 1824 (1997).
[25] T. Fujii, N. Sakata, J. Takada, Y. Miura, Y. Daitoh, and M. Takano, J. Mater. Res. **9**, 1468 (1994).
[26] L. Smart and E. Moore, *Solid State Chemistry, An Introduction* (Chapman and Hall, London, 1992), pp. 95–96.
[27] R. N. Blumenthal and D. H. Whitmore, J. Electrochem. Soc. **110**, 92 (1963).
[28] D. C. Cronemeyer, Phys. Rev. **87**, 876 (1952).
[29] D. C. Cronemeyer, Phys. Rev. **113**, 1222 (1959).
[30] W. Göpel, G. Rocker, and R. Feierabend, Phys. Rev. B **28**, 3427 (1983).
[31] J. Maserjian and C. A. Mead, J. Phys. Chem. Solids **28**, 1971 (1967).
[32] Y. Katsuta, A. E. Hill, A. M. Phahle, and J. H. Calderwood, Thin Solid Films **18**, 53 (1973).
[33] E. M. Logothetis and W. J. Kaiser, Sens. Actuators **4**, 333 (1983).
[34] Y. Fukuda, K. Numata, K. Aoki, A. Nishimura, G. Fujihashi, S. Okamura, S. Ando, and T. Tsukamoto, Jpn. J. Appl. Phys., Part 2 **37**, L453 (1998).
[35] R. Swanepoel, J. Phys. E **16**, 1214 (1983).
[36] X. M. Lu, J. S. Zhu, W. Y. Zhang, G. Q. Ma, and Y. N. Wang, Thin Solid Films **274**, 165 (1996).
[37] C. V. R. Vasantkumar and A. Mansingh, *Seventh IEEE International Symposium on Application of Ferroelectrics* (IEEE, New York, 1990), pp. 713–716.
[38] W. A. Harrison, *Electronic Structure and Properties of Solids* (Freeman, San Francisco, CA, 1980), pp. 438–452.

[This article is copyrighted as indicated in the article. Reuse of AIP content is subject to the terms at: http://scitation.aip.org/termsconditions. Downloaded to] IP: 140.113.38.11 On: Thu, 01 May 2014 07:41:17